Electron-Rich Rods as Building Blocks for Sb Strips and Te Sheets

Garegin Papoian*,† and Roald Hoffmann*,‡

Contribution from the Department of Chemistry and Biochemistry, University of California at San Diego, 9500 Gilman Drive, La Jolla, California 92093-0371, and Department of Chemistry and Chemical Biology and Materials Science Center, Cornell University, Ithaca New York 14853-1301

Received September 18, 2000. Revised Manuscript Received April 27, 2001

Abstract: We analyze the bonding in a number of networks of heavy main group elements comprised of finite-length linear chains fused at right angles. Isolated linear chain building blocks may be understood easily by analogy with three-orbital four-electron "hypervalent" bonding picture in such molecules as I_3^- and XeF_2. After deriving the appropriate electron-counting rules for such linear units, we proceed in an *aufbau* to fuse these chains into simple (and not so simple) infinite networks. It is proposed that (a) infinite Sb_3 ribbons of vertex sharing squares are stable for an electron count of 20 electrons per three atoms (i.e., Sb_3^{5-}); (b) sidewise fused Sb double ribbons are stable for an electron count of 38 electrons per six atoms (i.e., Sb_6^{8-}); (c) Sb_4 strips cut from a square lattice are stable at the electron count of 24 electrons per four atoms (i.e., Sb_4^{4-}); (d) Te_6 defect square sheets are stable at the electron count of 40 electrons per six atoms (i.e., Te_6^{4-}). The electronic structures of the solid-state compounds containing these networks, namely $La_{12}Mn_2Sb_{30}$, α-$ZrSb_2$, β-$ZrSb_2$, Cs_3Te_{22}, and Cs_4Te_{28}, are elaborated. We propose preferred electron counts for two hypothetical Sb ribbons derived from the Sb_3 ribbon in $La_{12}Mn_2Sb_{30}$. A possibility of geometry distortion modulation by excess charge in lattices comprised of even-membered linear units is suggested.

1. Introduction

Classical Zintl−Klemm ideas have been fertile in rationalizing and predicting the crystal structures and chemical and physical properties of innumerable solid-state compounds. Many phases containing main group elements conform well to these rules, which derive from the octet rule in molecular chemistry. For instance, NaTl is the classical Zintl−Klemm compound—an electron is transferred from electropositive Na to Tl, the resulting Tl^- acquiring bonding properties characteristic of group fourteen elements and forming a diamond net.[1]

While the structures of most compounds of late heavy main group elements such as Sb and Te conform to Zintl−Klemm electron-counting rules, we have recently pointed to a large number of elemental, binary, ternary, and quaternary phases where an alternative and modified electron-counting scheme is required to rationalize the bonding in them.[2] Thus, infinite linear chains are stable for an electron count of seven electrons per atom, square sheets for six electrons per atom, and a cubic lattice for five electrons per atom.[2] We have also proposed magic or preferred electron counts for a number of other main group element networks which may be derived from linear chains and square sheets. Our analysis shows that there is a direct connection between bonding in these delocalized infinite networks and the well-known concept of hypervalent bonding for molecular compounds.

The linear chains, square sheets and other more complicated related networks have something in common—the σ-bonding framework for these lattices is so delocalized that it does not make much sense to discuss individual bonds; the band structure formalism is the most appropriate (see our earlier work for more detailed analysis[2]). However, hypervalent bonding occurs in the solid state in the completely localized form as well, an obvious example being the I_3^- anion surrounded only by cations. For compounds with localized hypervalent bonding the Zintl−Klemm electron-counting rules need to be modified only slightly, to take into account the appropriate number of electrons characteristic of isolated hypervalent molecules instead of the number dictated by the classical octet rule.

There is yet another group of main group element networks which are *intermediate* in their bonding picture between the completely delocalized bonding in linear chains and square sheets and localized hypervalent bonding in molecules such as I_3^- and XeF_2. Although the corresponding σ-framework orbitals broaden significantly into bands in these lattices, the underlying hypervalent molecular orbitals are still recognizable and serve as useful predictors of stability.[3] At first glance these networks might seem to be unrelated to each other. However, they all may be constructed in a systematic *aufbau* from finite-length linear chains fused in an appropriate way. The goal of this paper is illustrate how one may develop electron-counting rules for various networks derived from finite-length linear rods. Our starting point is the well-understood picture of three-orbital four-electron hypervalent bonding in molecular compounds, which we generalize to longer chains. Once these are in hand, we show how to construct various networks by fusing these chains together and properly taking into account the change in the number of electrons which ensues on fusion.

We use several solid-state compounds of Sb and Te to illustrate our ideas. The bonding in some of these compounds has been studied earlier in other contexts by us, as well as by others, however, we illustrate in this paper a novel, heuristically

‡ Cornell University.
† University of California at San Diego.

(1) Miller, U. *Inorganic Structural Chemistry*; John Wiley & Sons, Inc.: New York, 1992.
(2) Papoian, G. A.; Hoffmann, R. *Angew. Chem., Int. Ed.* **2000**, *39*, 2408.
(3) Papoian, G.; Hoffmann, R. *J. Solid. State Chem.* **1998**, *139*, 8.

10.1021/ja003420x CCC: $20.00
Published on Web 06/15/2001

useful approach to understanding these materials.[2−7] We start by analyzing the electronic structure of a one-dimensional Sb ribbon of vertex-sharing squares found in $La_{12}Mn_2Sb_{30}$.[8] Similar ribbons fuse sidewise into wider strips in the α-$ZrSb_2$structure, which we discuss next, along with Sb_4 ribbons found in the β-$ZrSb_2$ crystal structure. Finally, we illustrate how the relatively complicated Te subnetwork in the Cs−Te binary phases may be rationalized as Te_5 rods fused in a simple way to form two-dimensional defect square sheets.

2. The Electronic Structure of Simple Finite Linear Chains

The analysis of the electronic structure of finite linear chains of heavy main group elements is facilitated by the absence of strong s−p mixing for these elements, as well as the relative unimportance of π-bonding.[2,9] An underlying assumption in our analysis, based on much experience, is that for a chemical species to be stable, its bonding and nonbonding molecular orbitals must be filled while strongly antibonding molecular orbitals must be empty. The necessity for filling weakly antibonding orbitals depends on a particular system; but these may be filled as well.

Since there is relatively little s−p mixing for such elements as Sb and Te, it is reasonable to consider the lower-lying s-orbital as a lone-pair (a detailed analysis of the role of s−p mixing is given elsewhere[2]). The p-orbitals perpendicular to the linear chains (p_x and p_y in **1** if the chain is propagated along the *z*-axis) are engaged in π interactions which by being weak for heavy elements introduce a relatively small splitting between π-bonding and π-antibonding levels. It turns out that these weakly antibonding orbitals are low enough in energy that they are almost always populated. Therefore, one may consider the perpendicular p_x and p_y orbitals as lone pairs as well.

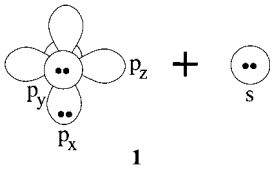

1

The reasoning above leads us to the conclusion that only p_z orbitals are responsible for the bonding interactions which hold the linear chain together. The bonding scheme for a three-membered linear chain, such as in $I_3^-$and XeF_2 was addressed very early in the literature by Pimentel and Rundle,[10,11] and has become known as electron-rich three-center or hypervalent bonding.[12,13] According to this scheme three p_z orbitals in a linear triatomic molecule split into bonding, nonbonding, and antibonding molecular orbitals (see **1**). If the first two molecular orbitals are filled with electrons, this results in a total of $6 \times 3 + 4 = 22$ electrons per molecule, which is consistent with the number of electrons in I_3^- and XeF_2. This picture of four-electron three-orbital bonding is an oversimplification since some mixing with the lower-lying s-orbitals does occur. However, this additional mixing does not lead to any critical changes.

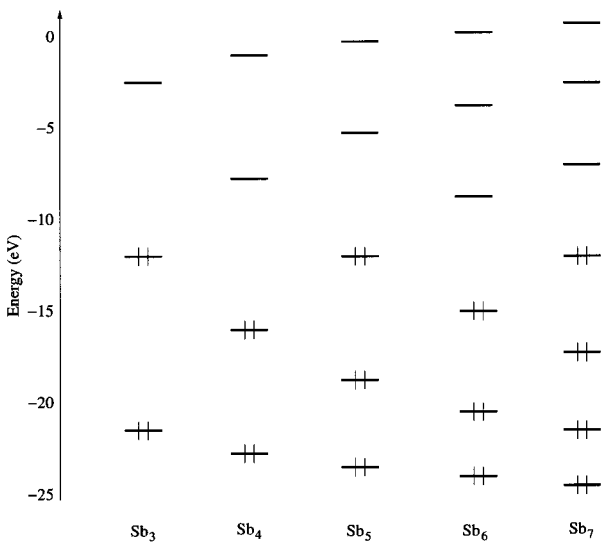

Figure 1. Hückel energy level diagram for the MOs derived from the p_z orbitals in linear equidistant Sb chains (Sb−Sb 3.0 Å)

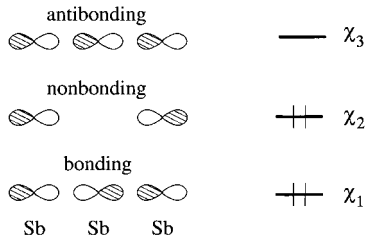

2

The description of the electronic structure for longer odd-numbered finite linear chains parallels that for a triatomic unit. The s and p_x and p_y orbitals are lone pairs, while the p_z orbitals split into a group of equally numbered bonding and antibonding molecular orbitals and a single nonbonding (actually, weakly antibonding due to mixing with s) molecular orbital (Figure 1). For even-membered chains the molecular orbital splitting pattern for the p_z orbitals is topologically different—all orbitals are either bonding or antibonding (Figure 1). Therefore, even-membered linear chain atoms may carry only one electron per p_z orbital while their odd-membered counterparts may carry additional electrons ($(n + 1)/n$ electrons per p_z for an *n*-membered chain).

If one were to construct extended networks using linear chains as building blocks, the different electron counts for odd and even membered linear chains would imply different electron counts for these networks as well. In the next three sections we are going to explore the electronic structure of various strips and sheets that contain three-, four-, and five-membered finite linear chains as their basic building blocks

3. One-Dimensional Sb_3 Ribbons

One-dimensional Sb_3 ribbons of vertex-sharing Sb squares found in the antimony sublattice of $La_{12}Mn_2Sb_{30}$[8] may be thought of as a collection of fused Sb_3 finite linear units (see **3**); thus, they serve as a good starting point for our analysis. In the actual structure, the ribbons undergo a sliding distortions of the central Sb atoms (**3a**), while here we consider only idealized ribbons (**3b**). The electronic effects behind the second-

(4) Böttcher, P. *Angew. Chem., Int. Ed. Engl.* **1988**, *27*, 759.
(5) Brylak, M.; Jeitschko, W. *Z. Naturforsch. B: Chem. Sci.* **1994**, *49*, 747.
(6) Brylak, M.; Möller, M.; Jeitschko, W. *J. Solid State Chem.* **1995**, *115*, 305.
(7) Nesper, R. *Prog. Solid State Chem.* **1990**, *20*, 1.
(8) Sologub, O.; Vybornovand, M.; Rogl, P.; Hiebl, K.; Cordier, G.; Woll, P. *J. Solid. State Chem.* **1996**, *122*, 262.
(9) W. Kutzelnigg. *Angew. Chem., Int. Ed. Engl.* **1984**, *23*, 272.
(10) Pimentel, G. C. *J. Chem. Phys.* **1951**, *19*, 446.
(11) Rundle, R. E. *J. Am. Chem. Soc.* **1963**, *85*, 112.
(12) Musher, J. I. *Angew. Chem., Int. Ed. Engl.* **1969**, *8*, 54.
(13) The word "hypervalent" makes some people see red. We think it is a useful descriptor for electron-rich multicenter bonding, and we use it as synonymous for such bonding.

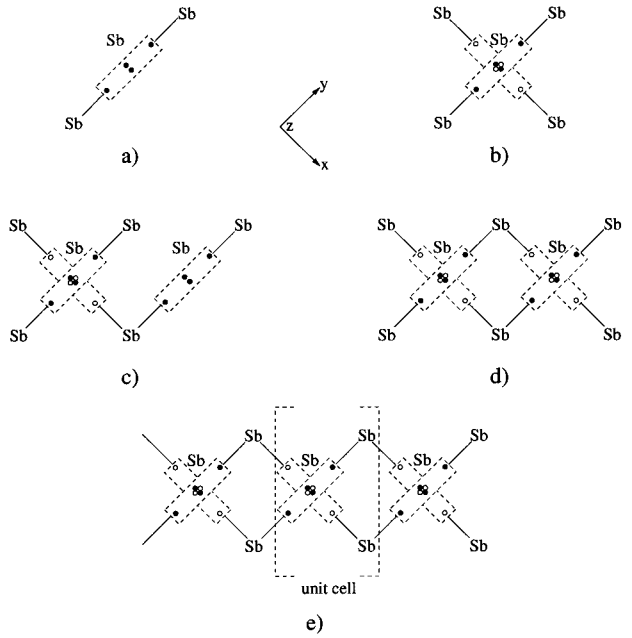

Figure 2. Hypothetical build-up process of Sb_3 ribbons from triatomic linear units. In addition to the electrons shown, each Sb possesses four electrons in s and p_z lone pairs. For molecules (a−c) some of the Sb atoms carry a p_x or p_y lone pair if those atoms are not engaged in bonding for the corresponding directions (for example, each Sb carries a p_x lone pair in a). Only electrons involved in three-center bonding are shown explicitly.

order Jahn−Teller interactions leading to the sliding distortion is given in our previous paper, here we only look at the electron counting in these ribbons.[3]

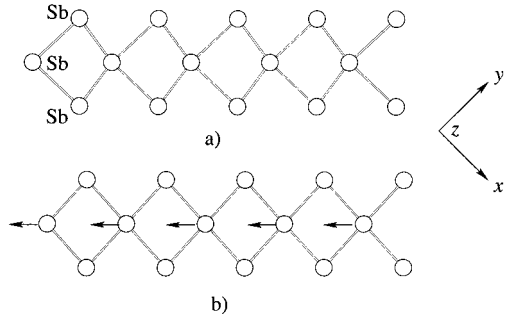

3

The aufbau process of constructing the Sb_3 ribbon from linear triatomic sticks is schematically depicted in Figure 2 (only "hypervalent" electrons are shown explicitly). Each Sb atom in Figure 2 possesses at least two lone pairs, s and p_z, while some Sb atoms carry an additional p_x *or* p_y lone pair if that particular orbital does not participate in three-center bonding. For instance, there are six electrons in p_x lone pairs in linear triatomic Sb_3 (Figure 2a) in addition to 12 electrons in s and p_z lone pairs. If four electrons involved in electron rich bonding, shown schematically in a box in Figure 2a, are added to these 18 electrons in lone pairs, then an electron count of $6 + 12 + 4 = 22$ electrons per Sb_3 molecule results, in agreement with the previous discussion.

Next, we consider fusing two linear Sb_3 molecules into an Sb_5 unit with a square coordination for the central atom (Figure 2b). In addition to $4 \times 5 = 20$ electrons in s and p_z lone pairs, there are also 8 electrons in p_x *or* p_y lone pairs for "ligand" or terminal Sb atoms (these lone pairs lie in the plane of the molecule and are perpendicular to the three-center bonds). Since another eight electrons participate in "hypervalent" bonding, there are overall $20 + 8 + 8 = 36$ electrons in this molecule, or Sb_5^{11-}. Notice, that classical hypervalent XeF_4 also has 36 valence electrons, that is, our derivation is internally consistent.

One may continue the build-up process in an incremental manner (Figure 2c−d), adding Sb_3 sticks on each step, counting lone-pair and hypervalent electrons along the way. The final result of such construction is the infinite Sb_3 ribbon. In the unit cell of three Sb atoms (Figure 2e), there are 12 electrons in s and p_z lone pairs, while there are no p_x and p_y lone pairs, as the latter all participate in three-center bonding. In addition, we should count eight "hypervalent" electrons per unit cell, bringing up to 20 the number of electrons per unit cell. This is, we believe, the magic electron count for infinite X_3 ribbons, where X is a heavy late main-group element. This electron count is consistent with the total number of electrons in the unit cell of $La_{12}Mn_2Sb_{30}$ as inferred from the preferred electron counts for the Sb sublattices in the structure as well as detailed band structure calculations.[3]

One geometric way to think about Sb_3 ribbons is to consider them as one of the most narrow strips cut from a square lattice.[14] Wider Sb strips are found in the binary Zr−Sb phases.[15−17] Electron-counting rules for these ribbons are discussed next.

4. Electronic Structure of $ZrSb_2$ Binary Phases

Binary and ternary Sb phases with transition metals are often hard to interpret. Behind this is the relatively small difference between the Sb and transition metal electronegativities. The oxidation states of the transition metal ions are often completely unknown from experimental work and are difficult to assess theoretically. We wish to show that for some specific intermetallic phases we can pull out and study isolated classical or electron-rich subnetworks. The nature of the bonding in an isolated subnetwork is then a reasonably good starting point for the subsequent analysis of the total structure.

The $ZrSb_2$ binary phases are intermetallic compounds in which the electronic fingerprints of the isolated Sb subnetworks are not destroyed much in the total structure. The crystal structure of α-$ZrSb_2$ was reported by Kjekshus.[15] Later Garcia and Corbett[16,17] carried out comprehensive experimental and theoretical studies of various Zr−Sb binary phases. Since we are interested in electron-rich Sb networks, in the subsequent discussion we are going to focus only on two Zr−Sb phases—α-$ZrSb_2$ and *β*-$ZrSb_2$. Our own analysis is complementary to the important work of Garcia and Corbett.[17]

4.1. Where Are the Extra Electrons in α-ZrSb2? A perspective view of the α-$ZrSb_2$ crystal structure and the Sb_6 strip is given in Figure 3, a and b. There are two Sb sublattices in the structure, Sb_2 pairs and Sb_6 strips, in the ratio $Zr_8(Sb_2(pair))_2(Sb_6(strip))_2$ The Sb_6 strip can be imagined as constructed from two Sb_3 strips, which we have already examined (see **3**).

We determined that the optimal electron count for a one-dimensional Sb_3 strip is 20 electrons per unit cell, that is, Sb_3^{5-}. What happens to the electron count when two strips are brought close to each other sidewise (Figure 3b)? Since lone pair − lone pair interactions are expected to be repulsive, one should remove an electron from each edge Sb lone pair in order to form a bond between two ribbons (cf. **4**). Taking into account

(14) Another narrow strip, the simple ladder, has been discussed by us in ref 2.

(15) Kjekshus, A. *Acta Chem. Scand.* **1972**, *26*, 1633.
(16) Garcia, E.; Corbett, J. *J. Solid State Chem.* **1988**, *73*, 440.
(17) Garcia, E.; Corbett, J. *J. Solid State Chem.* **1988**, *73*, 452.

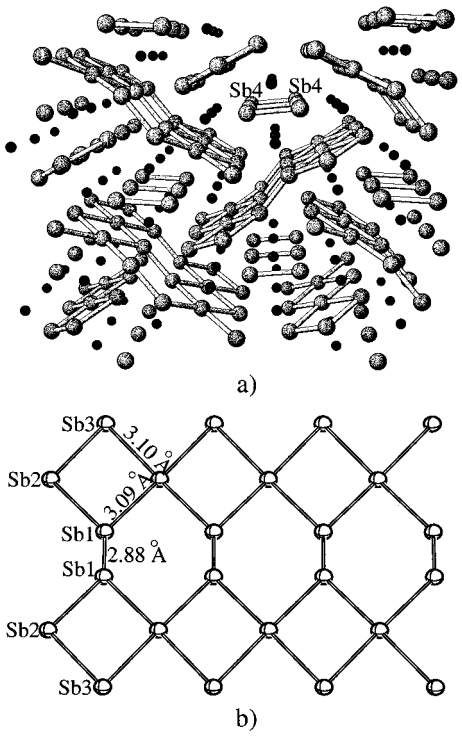

Figure 3. (a) Perspective view of $ZrBb_2$ (α-$ZrSb_2$-type) crystal structure. Zr: small dark spheres. Sb: large light sphere. (b) A perspective view and selected distances in Sb_6 strips.

the loss of two electrons per unit cell, the resulting electron count is Sb_6^{8-}.

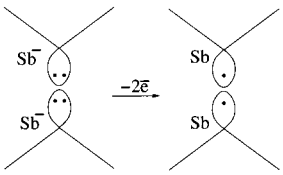

4

There exists another Sb substructure in α-$ZrSb_2$, one consisting of isolated Sb_2 pairs with a long (3.07 Å) Sb−Sb bond (Sb4 in Figure 3a). If one were to assume a single bond between these two Sb's, and complete an octet around each, a 4− charge would be assigned to the Sb_2 unit. The eight formula units in the α-$ZrSb_2$ unit cell (Zr_8Sb_{16}) can be broken down as $Zr_8(Sb_6\text{-}(strip))_2(Sb_2(pair))_2$. Following our qualitative reasoning, the overall charge on the Sb network is $2 \times (8-) + 2 \times (4-) = (24-)$. If we further assume that Zr is 4+ (Zr_8^{32+}), then there remain eight unaccounted electrons in the unit cell. At this point, without doing any calculations, we can only say that, when Zr_8^{32+}, Sb_{12}^{16-} (strips), and Sb_4^{8-} (pairs) are brought together, something will be reduced by eight electrons.

The description of bonding in α-$ZrSb_2$ is significantly complicated by the existence of many Zr−Sb bonding states near the Fermi level.[17] The closest Zr−Zr contacts are at 3.42 Å, a distance much longer than found typically for a Zr−Zr bond. However, our computed Zr−Zr overlap populations (discussed below) are indicative of weak bonding interactions. The additional eight electrons can enter Zr lone pairs, Zr−Sb bonding states, and/or Zr−Zr weakly bonding states, or Sb_2 pair Sb−Sb antibonding states, or Sb_6 strip Sb−Sb antibonding states. Where do these additional electrons end up?

The changes in atomic charges, as computed from a Mulliken population analysis, provide us with the initial clue about the reduction process. When eight electrons are added to $Zr_8Sb_{16}^{8+}$, the overall charge on Zr atoms decrease by −5.35, on Sb pairs by −0.73, and on Sb strips by −1.91. Hence, there is a strong indication that Zr atoms are reduced, with formal oxidation states closer to +3 than to +4. These changes in the Zr Mulliken charges do not tell us whether the Zr nonbonding orbitals (lone pairs) or Zr−Sb bonding states become occupied. The same ambiguities remain for Sb pairs and Sb strips.

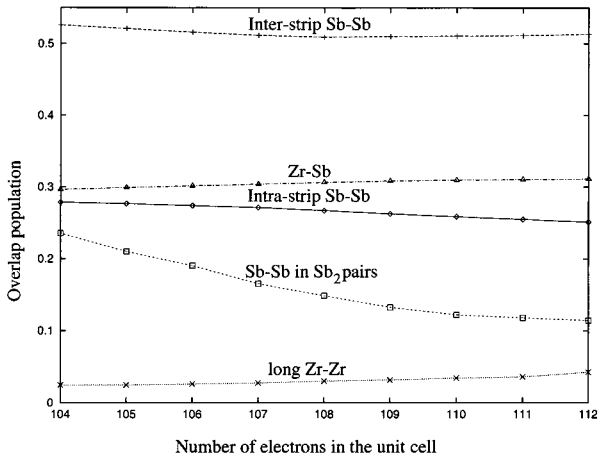

Figure 4. Various overlap population values in α-$ZrSb_2$ as a function of electron filling. The total number of electrons in the unit cell of charge neutral Zr_8Sb_{16} is 112. 104 electrons is the electron count for $(Zr^{4+})_8(Sb_6^{8-}(strip))_2(Sb_2^{4-}(pair))_2$.

We attempt to gain a deeper insight into the nature of the reduction by eight electrons with the help of fragment overlap population analysis.[18] The total number of electrons in the system may be partitioned into the sum of intra-fragment and inter-fragment overlap populations. Following this procedure, we have found that out of eight electrons added to $Zr_8Sb_{16}^{8+}$, 4.79 enter Zr lone-pair bands, 1.12 enter Zr−Sb bonding states, and 2.11 enter the Sb subnetwork.

We calculated also within the rigid band approximation various overlap populations in composite α-$ZrSb_2$ as a function of electron filling by the last eight electrons (Figure 4). The overlap population for the long 3.42 Å Zr−Zr contacts is enhanced by more than 50% upon the addition of eight electrons to the unit cell (Figure 4), but its absolute value remains very low. The initially large Zr−Sb overlap population is further enhanced by approximately 5% (Figure 4). Zr nonbonding states along with the Zr−Sb states serve as the largest sink for those eight electrons. Using the overlap population analysis for various bonds we estimate that (1) the formal oxidation state of Zr is much closer to 3+ than to 4+ and (2) the Sb_2^{4-} pairs and the Sb_6^{8-} are reduced by 2.11 electrons. Our results, although from a somewhat different prospective, are not inconsistent with the work of Garcia and Corbett.[17]

An unexpected consequence of adding eight electrons is the partial reduction of Sb_2^{4-} pairs by 0.23 electron per one pair. One would expect all extra electrons in the Sb sublattice to be accommodated by low-lying unoccupied bands of hypervalent Sb_6 strips. Why does the high-lying antibonding σ^* band of the classical Sb_2^{4-} unit get partially filled? Garcia and Corbett[17] noticed a sharp Sb_2 pair antibonding peak in COOP just below the Fermi level. This sharp peak (Figure 5a), which we attribute to the σ^* antibonding band, is situated *above* the Fermi level in the isolated Sb sublattice. When the latter sublattice interacts

(18) Glassey, W.; Papoian, G.; Hoffmann, R. *J. Chem. Phys.* **1999**, *111*, 893.

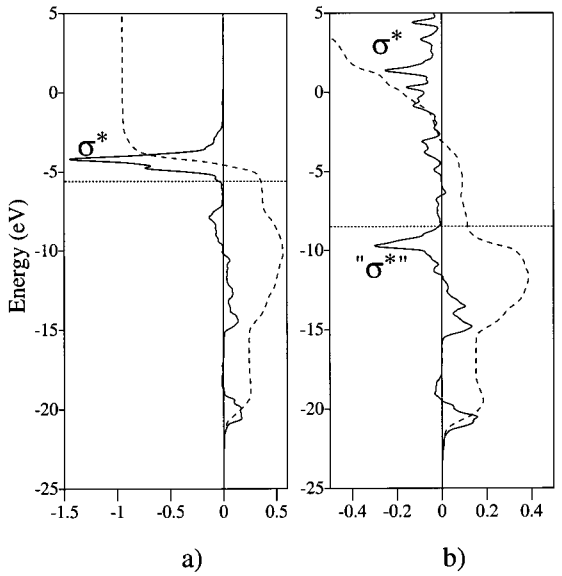

Figure 5. Sb−Sb COOP (solid line) and its integration curve (broken line) for the interaction in Sb_2 pairs in (a) the isolated Sb sublattice, taken from α-$ZrSb_2$, with the electron count corresponding to Sb_{16}^{24-}, and (b) the full crystal structure of α-$ZrSb_2$.

with the Zr sublattice, the main body of the σ^* peak is strongly pushed up and dispersed, due to the interaction with the Zr bands, as would have been anticipated. But the same interaction produces a satellite peak (Figure 5b), more than 5 eV below the original σ^* peak. Since this satellite peak is below the Fermi level in the calculation of the α-$ZrSb_2$ crystal structure, its population by electrons weakens the Sb−Sb bonding in Sb_2 pairs. But it does not break it entirely.

This satellite peak can be attributed to an unusual, concentrated coupling of the original σ^* band with the Zr d-bands. To understand this coupling, we modeled the Sb_2 pair environment in α-$ZrSb_2$ by molecular Sb_2Zr_8(**7a**). As for the extended case, the σ^* orbital is mostly pushed up and is dispersed due to the interaction with Zr. But we find an analogous low-lying molecular orbital, corresponding to the coupling in the extended structure; that molecular orbital is depicted in **5b** (Sb's are black central atoms in **5a**).

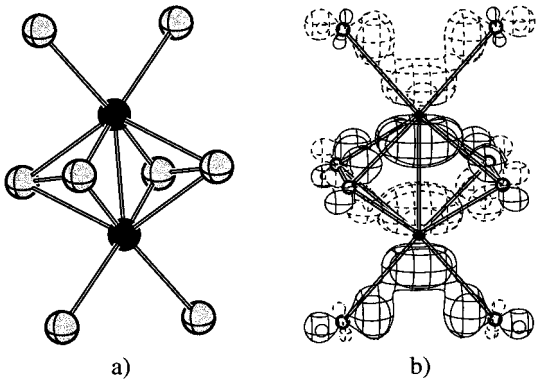

5

Despite the intermetallic nature of α-$ZrSb_2$ it is possible to analyze individual classical Zintl and hypervalent Sb subnetworks, then reassemble them back into the total crystal structure. The hypervalent electron-counting scheme developed for Sb_3 strips has served as a valuable starting point for this analysis. Unfortunately, no such starting point exists yet for the description of bonding in Sb_4 strips in β-$ZrSb_2$. This is the next topic which we take up.

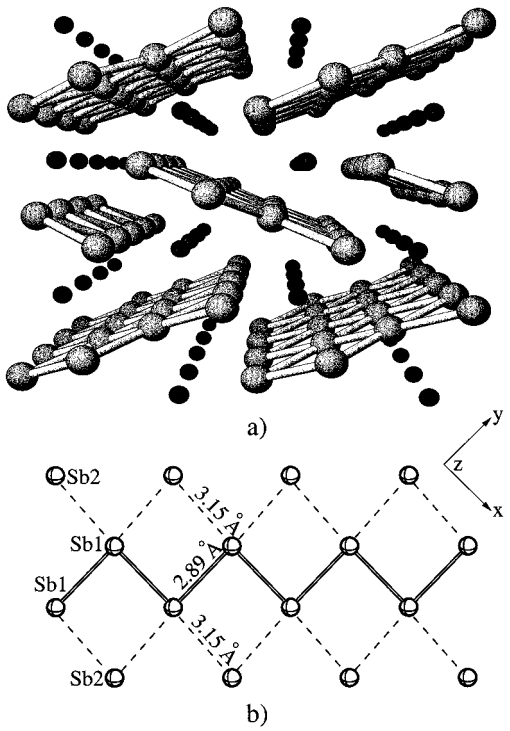

Figure 6. (a) Perspective view of β-$ZrSb_2$ crystal structure.[17] Zr: small dark spheres. Sb: large light spheres. (b) Perspective view and selected distances in Sb_4 strips.

4.2. Electronic Structure of β-$ZrSb_2$. At first glance the crystal structure of β-$ZrSb_2$ (Figure 6a) appears to be simpler than the one of α-$ZrSb_2$. This is perhaps true from the structural point of view, but the electronic structure of β-$ZrSb_2$ is quite involved. Behind this are nontrivial secondary interactions between Sb2 and Sb1 in one-dimensional Sb_4 strips (Figure 6b). One can approach these strips from two extreme viewpoints. In one case one assumes no interaction between side and central atoms in the strips. Alternatively, one may think of the Sb_4 strip in Figure 6b as being derived from a more symmetrical strip with equal Sb1−Sb1 and Sb1−Sb2 distances. These two conceptual fragmentations lead to different charges on the Sb lattice. This is the main source of our complications.

Under the first assumption of isolated Sb2 atoms and isolated Sb1 zigzag chains, a 3− charge is assigned to Sb2 atoms and a 1− charge is assigned to Sb1 atoms. Taking into account the crystal site multiplicities, the charges in β-$ZrSb_2$ can be formally assigned as $Zr^{4+}Sb^{1-}Sb^{3-}$. Garcia and Corbett[17] noticed that this simple Zintl picture is not completely consistent with metallic properties of β-$ZrSb_2$—they suggest an important role for Zr−Sb bands. Our calculations indicate the electronic structure of β-$ZrSb_2$ is significantly altered from the $Zr^{4+}Sb^{1-}Sb^{3-}$ formulation due to strong Sb2−Sb1 interactions. Therefore, we proceed next to estimate the electron count for a symmetrical Sb_4 strip, cut from an ideal square lattice.

If the Sb_4 strip lies in the *xy* plane, then assuming once again weak π-bonding and weak s−p mixing, we fill completely lower-lying s and p_z lone pairs. We have chosen the direction of *x* and *y* axes in such a way (see Figure 6b), that they point toward Sb−Sb bonds in the Sb_4 strip. Each atom in the strip is involved in two four-center bonding patterns both in *x* and *y* directions.

As we noted, even-membered chains have different molecular orbital patterns than those of the odd-membered ones (Figure

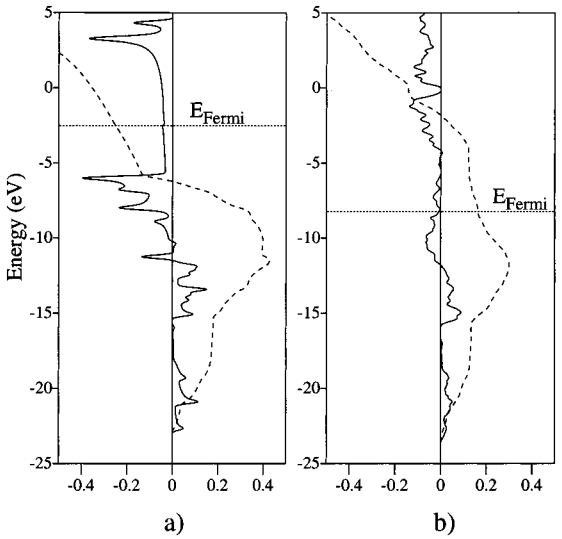

Figure 7. Sb1−Sb2 COOP (solid line) and its integration curve (broken line) for the interaction in (a) the isolated Sb sublattice, taken from β-$ZrSb_2$, with the electron count corresponding to Sb_4^{8-}; (b) the full crystal structure of β-$ZrSb_2$.

1). For example, the three-orbital interaction (see 2) produces bonding, nonbonding, and antibonding orbitals. On the other hand, the four-orbital basis leads to two bonding and two antibonding orbitals (see **6**). Therefore, electron filling by four electrons (*one electron per atom*) should be strongly favored over filling by six electrons, when one of the antibonding orbitals becomes filled. In the Sb_4 strip of β-$ZrSb_2$each Sb is involved in two four-center bonds (*x* and *y* directions); therefore, each Sb should possess six electrons ($2(s) + 2(p_z) + 1(p_x) + 1(p_y)$), making it Sb^{1-}. Accordingly, the charges in β-$ZrSb_2$ should be written formally as $Zr^{2+}Sb1^{1-}Sb2^{1-}$. The band structure of the isolated Sb_4 strip (not shown here) is consistent with the electronic description just made.

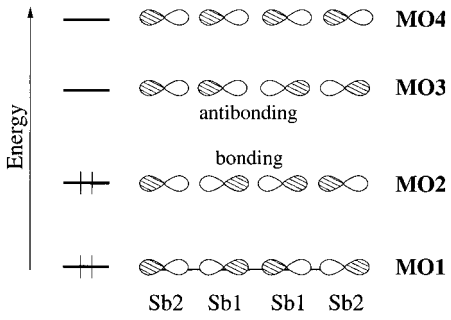

6

We see that, if there are no Sb1−Sb2 interactions, then the charge on the Sb subnetwork forces a 4+ formal oxidation state on Zr. On the other hand, when Sb1−Sb2 interactions are as strong as Sb1−Sb1 interactions, then Zr is reduced to 2+. Starting from the $Zr^{4+}Sb^{3-}Sb^{1-}$ formulation, we can imagine that as the Sb1−Sb2 interactions are gradually turned on, bands related to MO3 in **7** are pushed up until at some point they dump their electrons into the Zr levels. The Sb1−Sb2 COOP for the isolated Sb_4^{8-} strip taken from β-$ZrSb_2$ is given in Figure 7a. For the Fermi level determined for this charge, the Sb1−Sb2 overlap population is a negative number (−0.25), consistent with our analysis (the bands corresponding to antibonding MO3 in **7** are filled and overcome the bonding in the lower occupied levels). When the Zr^{4+} ions are introduced into the isolated Sb sublattice (Figure 7b), the Fermi level dramatically drops, resulting in a positive Sb1−Sb2 overlap population (0.16), which is still less than 0.33 in Sb_4^{4-}(antibonding bands corresponding to MO3 completely empty). The Sb1−Sb1 overlap population also becomes enhanced when Zr^{4+} ions interact with the Sb sublattice in β-$ZrSb_2$.

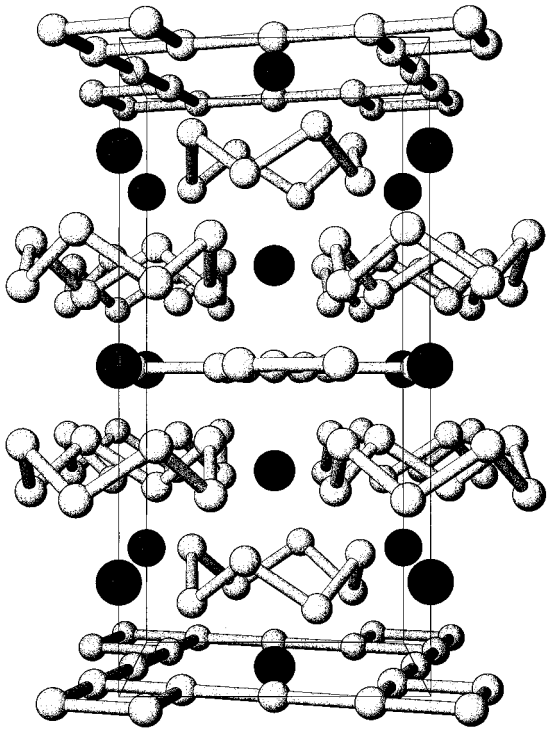

Figure 8. Perspective view of the Cs_3Te_{22} crystal structure. Cs: large dark spheres. Te: smaller light spheres.

Taking into account the previous results, we conclude that the combination of Zr^{4+} and $Sb^{3-}Sb^{1-}$ into a single-crystal structure leads to a significant backflow of electron density to the Zr sublattice (mainly to Zr−Sb states[17]). The oxidation state of Zr is, therefore, intermediate between 4+ and 2+.

Next we consider two-dimensional defect Te square lattice in the binary Cs_3Te_{22} phase which can also be thought of as being comprised from now *five-membered* linear chains.[19,20]

5. Unusual Te Networks in Cs−Te Binary Phases

The beautiful crystal structure of the Te-rich Cs_3Te_{22} binary phase was reported by Sheldrick and Wachhold (see Figure 8).[19] Two noninteracting Te substructures coexist in Cs_3Te_{22}, Te_8 isolated crown-shaped rings and Te_6 two-dimensional nets.[19,21] It is safe to assume the neutrality of Te atoms in Te_8 rings, since each Te is classically bonded to two other Te atoms (detailed arguments for the charge assignment and bonding are given in ref 22). As there are six sheet Te atoms in the Te_{22} formulation, we are led to a 3− charge on the Te_6 sheets: $(Cs_3^{3+}[Te(crown)_{16}]^0[Te(sheet)_6]^{3-})$.

Liu, Goldberg, and Hoffmann (see also Jobic and coworkers[23]) have analyzed in detail the bonding in Te_6^{3-} sheets using a band-structure formalism.[22] Since the Te atoms in this sheet are found in a locally linear or T-shaped arrangement, one would expect that the hypervalent bonding ideas would be

(19) Sheldrick, W. S.; Wachhold, M. *Angew. Chem., Int. Ed. Engl.* **1995**, *34*, 450.
(20) Sheldrick, W. S.; Wachhold, M. *Chem. Commun.* **1996**, p 607.
(21) Kanatzidis, M. G. *Angew. Chem., Intl. Ed. Engl.* **1995**, *34*, 2109.
(22) Liu, Q.; Goldberg, N.; Hoffmann, R. *Chem. Eur. J.* **1996**, *2*, 390.
(23) Jobic, S.; Sheldrick, W. S.; Canadell, E.; Brec, R. *Bull. Soc. Chim. Fr.* **1996**, *133*, 221.

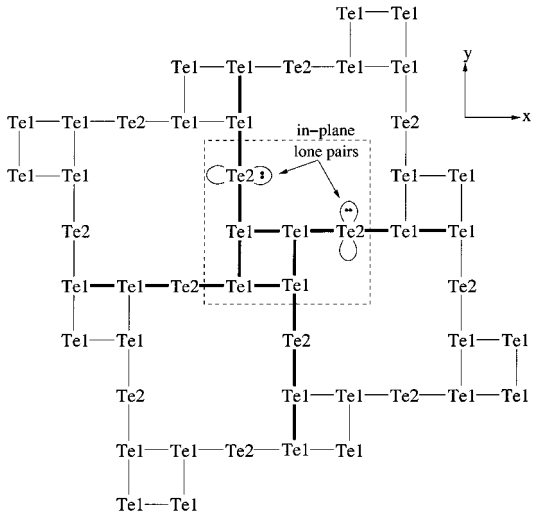

Figure 9. Two-dimensional Te network in Cs_3Te_{22}.

helpful in determining the optimal electron count for those sheets. As may be seen in Figure 9, there are two types of Te found in Te_6 sheets: Te1 being three-coordinated and Te2 being two-coordinated. Defocusing from the obvious squares in the structure, one may also view the Te_6 sheet as comprising Te_5 linear units crossing each other at right angles. We take this structural hint, analyze the bonding for isolated Te_5 units and then combine them into a two-dimensional sheet.

Five-membered linear chains were briefly encountered when deriving the optimal electron count for finite linear chains. Consistent with that previous discussion, we assume a low-lying s lone pair and two p lone pairs (p-orbitals perpendicular to the chain direction (see **7**). Next we populate all σ molecular orbitals except the antibonding ones: due to 2:1:2 splitting of σ-levels, six electrons are needed (see schematic drawing **8**). Therefore, to derive the preferred electron count for this two-dimensional network, one should multiply by six the number of five-center bonds per unit cell and add to that the number of lone pair electrons.

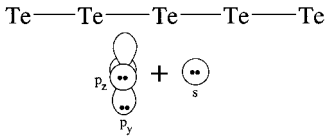

7

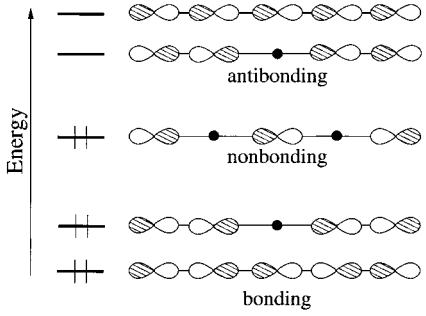

8

One observes in Figure 9 that four five-center bonds emanate from each unit cell, being shared, however, with neighboring unit cells. Thus, the two-dimensional Te net in Cs_3Te_{22} contains two five-center bonds per Te_6 unit cell, which in turn corresponds to $6 \times 2 = 12$ electrons residing in these delocalized bonds. In addition, each Te2 atom has an in-plane lone pair perpendicular to multicenter bonds, as shown in Figure 9. If $6 \times 4 = 24$ s and p_z lone pairs electrons are also taken into account, then one arrives at the $12 + 4 + 24 = 40$ electrons per unit cell, which corresponds to the Te_6^{4-} formulation.

As mentioned earlier, the actual charge is one electron less, that is, Te_6^{3-}. We do not have (nor did earlier studies) an explanation of why the system chooses to be slightly oxidized. Be that as it may, from the theoretical construction presented above, one would expect this electron to be removed from a band originating from the nonbonding σ-orbital (see **8**). Indeed, the band structure analysis of Te_6 sheets carried out by Liu, Goldberg, and Hoffmann indicated that the Fermi level crosses through the middle of a band which is derived from above-mentioned nonbonding σ-orbitals (actually, these orbitals are somewhat antibonding due to mixing with lower lying s-bands, as we have suggested several times in the earlier discussion).[22] Another remarkable feature of previous band-structure calculations is the presence of a wide band gap (about 2 eV) between the highest half-filled "nonbonding" hypervalent band and the remaining σ-antibonding bands.[22] This provides yet another justification for our frontier orbital approach of populating Te_5 molecular orbitals.

There is a yet simpler way to arrive at the Te_6^{4-} assignment. First, we notice that the optimal electron count for any odd-membered linear chain of a heavy main group element may be derived by breaking it into pairs and one isolated atom. For example, linear hypervalent I_3^- may thought of as being assembled from a classical I_2 pair and an isolated I^- atom. Similarly, if we break up a Te_5 unit into two side Te_2^{2-} pairs and a central Te^{2-} atom, the Te_5^{6-} assignment of charges results. For the Te_6 two-dimensional sheets we use isolated Te_4^0 squares and Te^{2-} atoms as building blocks, which leads to the -4 charge derived above (see **9**).

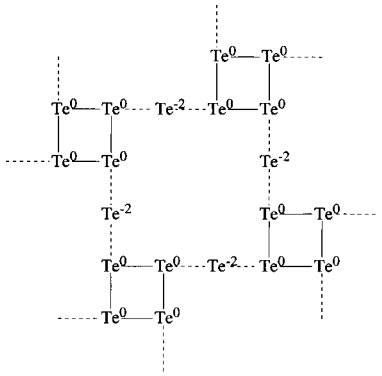

9

This line of reasoning works remarkably well for the Te network in the related Cs_4Te_{28} binary phase (Figure 10).[20] This nicely complicated compound contains Te_8 rings, Te_4 squares, and Te_6 helical chains $(Cs_4Te(ring)_8Te(square)_8Te(chain)_{12})$. Two ends of the latter chains (Te_6^{2-}) are engaged in strong secondary interactions (3.15 and 3.19 Å) with Te_4^0 squares so as to interlink the consecutive Te_6-like (as in Cs_3Te_{22}) two-dimensional sheets (see Figure 10). The interaction of lone pairs on bridging Te atoms with the Te_4^0 isolated squares may be described in exactly the same way as the previously considered interactions between lone pairs on isolated Te^{2-} atoms and Te_4^0 squares in Te_6^{4-} sheets (see **9**).

Unlike the Te_6 sheets in the Cs_3Te_{22} binary phase, the Te_{20}^{4-} network in Cs_4Te_{28} corresponds exactly to our hypervalent

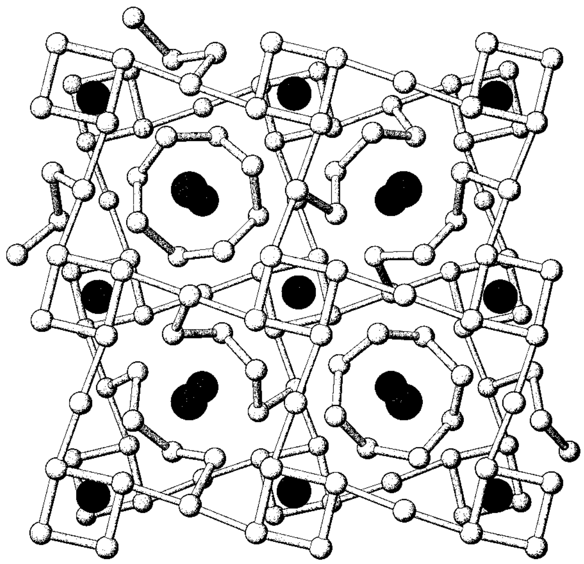

Figure 10. Perspective view of the Cs_4Te_{28} crystal structure. Cs: large dark spheres. Te: smaller light spheres.

formulation, that is, it is not oxidized by one electron. The difference between in-square Te−Te bonds and square Te−bridging Te bonds is somewhat higher in Cs_4Te_{22} (∼2.93 Å and ∼3.17 Å) than in Cs_3Te_{22} (∼3.00 Å and ∼3.08 Å). The reason for the greater distortion in the Te substructure in Cs_4Te_{22} is not immediately obvious. The crystal structures and patterns of bonding of Cs_3Te_{22} and Cs_4Te_{28} are closely related, as may be easily seen by comparing Figures 8 and 10, and as noted by the synthesizers of these beautiful compounds.

The bonding in the very unusual two-dimensional Te_6 sheet in Cs_3Te_{22} and the three-dimensional Te_{20} network in Cs_4Te_{28} is amenable to analysis with our hypervalent electron-counting ideas. For other aspects of bonding in these fascinating structures we refer readers to the earlier papers.[19−22]

6. Predicting Electron Counts for Hypothetical Networks

The electron-counting ideas put forward in this paper have been applied to a number of Sb ribbons and Te sheets, rationalizing the experimentally observed electron counts. Our theory possesses predictive power as well, with a potential to help solid-state chemists to design new electron-rich networks. Since one could propose an infinite number of one-, two-, and three-dimensional networks constructed from linear rods of different lengths, here we demonstrate only the application of our electron-counting scheme to two hypothetical one-dimensional ribbons related to the Sb ribbons discussed earlier.

The first ribbon which we propose (**10**) may be derived from the Sb_3 ribbon in $La_{12}Mn_2Sb_{30}$ (see **3a,b**) by adding an array of Sb atoms to each side of the Sb_3 ribbon. These atoms are marked as Sb^{III} in **10**. One may arrive at an infinite square lattice by repeatedly applying this construction. The translational unit cell in **10** contains five Sb atoms, thus we will refer to **10** as an Sb_5 ribbon.

To count electrons in the Sb_5 ribbon, we first notice that each Sb has s and p_z lone pairs, thus resulting in $5 \times 4 = 20$ lone pair electrons per unit cell. The remaining p_x and p_y orbitals form a delocalized σ-framework, which we approximate as a collection of noninteracting Sb_5 linear units (four Sb−Sb bonds per Sb_5 unit). Since we know that six electrons are needed for a stability of an isolated five-center electron-rich "bond" (see **8**), all we have to do is to count the number of such bonds per unit cell. There are eight bonding Sb−Sb contacts per Sb_5 unit cell (see **10**). Any five-center system contains four bonds. Thus, one has in this case a net total of $8/4 = 2$ such five center bonds. Therefore, $2 \times 6 = 12$ electrons per unit cell is the preferred electron count for the σ-framework of the Sb_5 ribbon, leading to the overall electron count of $20 + 12 = 32$ electrons per unit cell (i.e. $Sb^{-7/5}$).

Yet another hypothetical one-dimensional ribbon may be derived from the familiar Sb_3 ribbon (see **3b**) by adding Sb^{III} atoms to link alternatively neighboring central squares from above and below (see **11**). Although the resulting translational unit cell contains eight Sb atoms, one might consider as well a "helical" unit cell twice as small. In the following discussion we use the translational unit cell as a basis for electron counting, referring to it as an Sb_8 ribbon.

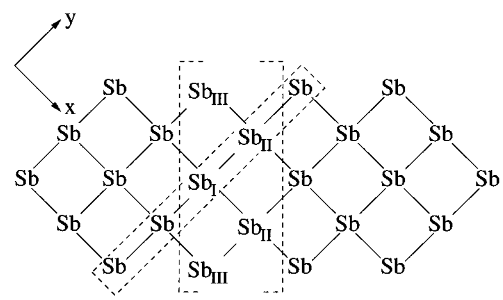

10

As in the previous example, we count first the lone pair electrons—there are $8 \times 4 = 32$ such s and p_z electrons per translational unit cell. As for the $p_x - p_y$ σ-framework, the situation is more interesting here. The electron-counting rules are different for odd-membered and even-membered rods (see the discussion in preceding sections). Although the parent Sb_3 ribbon (see **3b**) consists of three-membered rods, the Sb_8 ribbon is comprised of four-membered rods as its building blocks. Consequently, one expects four electrons in each of these four-center bonds (see **6**). Simple counting show that there are 12 Sb−Sb bonds in the Sb_8 ribbon unit cell, which in turn is equivalent to $12/3 = 4$ four-center bonds per unit cell (each four-center rod contains three Sb−Sb bonds). Therefore, $4 \times 4 = 16$ electrons are required for the stability of the σ-framework, bringing the total number of electrons to $32 + 16 = 48$ per unit cell (i.e., Sb^-, as in a simple square lattice[2]).

If the Sb_8 ribbon were to distort in a way reminiscent of the Sb_4 ribbon distortion in β-$ZrSb_2$ (Figure 6b) then Sb^{III}−Sb^{II} bond would stretch, resulting in the Sb_3 strip (**3b**) and nearly isolated Sb^{III} atoms (such a distortion would be the solid-state analogue of the second-order Jahn−Teller effect[3]). Since we have already determined that 20 electrons are needed per Sb_3 unit cell (40 for two unit cells), and eight electrons are required for the stability of an isolated Sb^{III} atom (16 for two atoms), then we arrive at $40 + 16 = 56$ electrons per Sb_8 unit cell (i.e., Sb^{2-}) for stability of the distorted version of ribbon **11**. We suggest

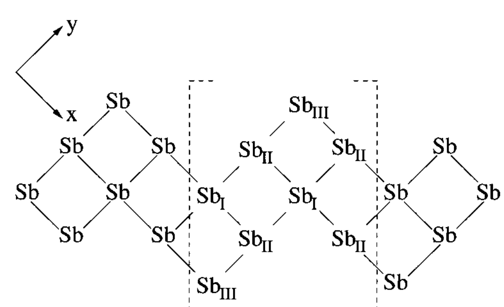

11

countercation substitution or designed nonstoichiometries could tune continuously this structural deformation (from undistorted Sb^- to highly distorted Sb^{2-}). Notice that equivalent distortions do not change the preferred electron counts for ribbons composed of odd-membered rings.

7. Conclusions

The concept of electron-rich or hypervalent bonding as applied to molecules such as I_3^-, XeF_2, PF_5 (and many others) has been recognized as most useful in the chemical community. It has also been used by our and other groups to analyze the electronic structure of solid state compounds having essentially zero-dimensional hypervalent units immersed into the matrix of other ions and networks. However, there exist many, seemingly unrelated, extended networks of heavy main group elements in hundreds of solid-state compounds which may be brought under a common roof using and extending the ideas of hypervalent bonding to infinite systems.[2] In our recent work we have demonstrated that infinite linear chains, square sheets, cubic lattices, and numerous other networks derived from these possess distinct electron counts which determine the structural stability of these networks.[2]

In the current work we have considered the electronic structure of infinite networks which exhibit a behavior intermediate between the completely localized hypervalent bonding in molecular compounds and completely delocalized bonding in infinite linear chains and square sheets. For instance, one-dimensional ribbons of vertex-sharing squares may be thought of as having two three-orbital four-electron bonds centered on central atoms. This analogy has allowed us to propose an electron count of 20 electrons per three atoms for these ribbons (Sb_3^{5-}), which is consistent with the overall number of electrons in $La_{12}Mn_2Sb_{30}$, where these ribbons are found.

Paired Sb_3 ribbons as well as isolated Sb_2 pairs are found in the α-$ZrSb_2$ crystal structure. When two isolated ribbons are brought sidewise together, a repulsion results due to interactions of side Sb lone pairs. To form inter-ribbon bonds, each side Sb must be oxidized by one electron, leading to the overall Sb_6^{8-} formulation for these ribbons. Assuming a -4 charge on the Sb_2 pairs and a $+4$ formal charge for Zr, one is led to the $Zr_8^{32+}Sb_{12}^{16-}$(strips)Sb_4^{8-}(pairs) assignment of charges, that is, eight electrons short from being charge neutral. Our fragment overlap population analysis suggests that there is a significant backflow of electrons to Zr and it is better to consider the latter as Zr^{3+}. We also have attributed the unusual elongation of the Sb−Sb bond in the Sb_2 pairs to the mixing of its σ^* orbital with the Zr d-orbitals and its subsequent population.

Sb_4 ribbons found in the β-$ZrSb_2$ are more difficult to analyze because of the even number of atoms in the linear chains which serve as building blocks. Two extreme viewpoints are possible for this material: (1) side Sb atoms do not interact with the middle Sb zigzag chain, leading to a $Zr^{4+}Sb^-$(zigzag)Sb^{3-}(isolated), and (2) the side and central interactions are similar, leading to a $Zr^{2+}Sb^{2-}$(strip). From our band-structure calculations it follows that there are significant interactions between the side atoms and the zigzag chain; the second formulation is a better description of bonding in this material.

Two-dimensional Te defect square sheets in the Cs−Te phases may also be thought of as comprising finite five-membered linear chains. When five-membered linear chains are fused to form a defect square sheet and the electron count is adjusted properly for this construction, one arrives at the Te_6^{4-} formulation. Compared to this result, it turns out that these sheets are oxidized by one electron in Cs_3Te_{22}; a nonbonding hypervalent band is oxidized. Te sheets are cross-linked into a three-dimensional structure by Te_6 helical chains in the related Cs_4Te_{28} binary phase. Our proposed electron count corresponds exactly to the total number of electrons for this material.

The systematic procedure which we have developed for reconstructing the electronic structures of one-dimensional ribbons and two-dimensional sheets may be applied not only to known phases $La_{12}Mn_2Sb_{30}$, α- and β-$ZrSb_2$ but also to design new lattices having linear chains as building elements. To illustrate this point we have proposed two one-dimensional Sb ribbons having five and eight atoms in the unit cell respectively which are related to the Sb_3 ribbon in $La_{12}Mn_2Sb_{30}$. For the Sb_5 ribbon, entirely comprised of five-center bonds, we have calculated a fractional charge of $-{}^7/_5$ per Sb atom ($Sb^{-7/5}$). As for the Sb_8 ribbon, composed of four-center bonds, we have suggested a -1 charge for the undistorted ribbon and -2 charge for the highly distorted geometry. Thus, we predict that networks assembled from even-membered linear chains may serve as charge reservoirs by accommodating or expelling an excess charge by a simple distortion.

In summary, short hypervalent linear chains of heavy main group elements serve as convenient building blocks for an *aufbau* of a number of seemingly unrelated extended networks. While the underlying "hypervalent" molecular orbitals broaden into bands in the extended systems, the latter still carry some memory of the molecular hypervalent bonding. One may develop electron-counting rules for a large number of extended networks by adjusting systematically the number of electrons when using hypervalent rods to construct these networks.

Acknowledgment. We gratefully acknowledge the National Science Foundation for its generous support of this work by Research Grant CHE-9970089 and the Cornell Theory Center for computer time. We thank the reviewers for encouraging us to make some predictions of magic electron counts (Section "Predicting Electron Counts for Hypothetical Networks").

Appendix I: Computational Details

All calculations were performed with the help of "Yet Another extended Hückel Molecular Orbital Package(YAeHMOP)", a program developed in our group by G. Landrum.[24] The standard atomic parameters were used for Sb and Zr. The parameters are listed in Table 1 with the corresponding references.

Table 1. Extended Hückel Parameters; the ζ's Are the Exponents of the Slater Orbital Basis Set, the c's the Coefficients in a Double-ζ Expansion

atom	orbital	H_{ii}(eV)	ζ_1	c_1	ζ_2	(c_2)	ref
Sb	5s	−18.8	2.323				25
	5p	−11.7	1.999				
Zr	5s	−9.87	1.817				26
	5p	−6.76	1.776				
	4d	−11.18	3.835	0.6210	1.505	0.5769	

JA003420X

(24) Landrum, G. A. http://overlap.chem.cornell.edu:8080/yaehmop.html, 1995.

(25) Hughbanks, T.; Hoffmann, R.; Whangbo, M.-H.; Stewart, K. R.; Eisenstein,O. E.; Canadell, E. *J. Am. Chem. Soc.* **1982**, *104*, 3876.

(26) Tatsumi, K.; Nakamura, A.; Hofmann, P.; Stauffert, P.; Hoffmann, R. *J. Am. Chem. Soc.* **1985**, *107*, 4440.